



Regular Paper

Hydraulic conductivity of bentonite-polymer geosynthetic clay liners to aggressive solid waste leachates

Dong Li^b, Hanrui Zhao^b, Kuo Tian^{a,*}^a Department of Civil, Environmental, and Infrastructure Engineering, George Mason University, Fairfax, VA, 22030, USA^b George Mason University, Fairfax, VA, USA

ARTICLE INFO

Keywords:

Bentonite-polymer (B-P)
 Geosynthetic clay liners (GCLs)
 Polymer type
 CCR leachate
 MSWI leachates
 MW leachate

ABSTRACT

Hydraulic conductivity of conventional mock sodium bentonite (Na-B) and bentonite-polymer (B-P) geosynthetic clay liners (GCLs) were evaluated with three synthetic leachates that are chemically representative of aggressive leachates from coal combustion product (CCR) ($I = 3179$ mM), mining waste (MW) ($I = 2127$ mM, $\text{pH} = 2.0$), and municipal solid waste incineration ash landfill (MSWI) ($I = 2590$ mM). The mock B-P GCLs were created by dry mixing bentonite with branched, linear, or crosslinked polymer. The polymer loading of mock B-P GCLs ranged from 3 to 15%. Comparative tests were also conducted with Na-B GCLs. The mock Na-B GCLs cannot maintain low hydraulic conductivity to aggressive CCR, MW, and MSWI leachates. Mock B-P GCLs with 10% branched polymer had low hydraulic conductivity ($< 1.0 \times 10^{-10}$ m/s) to synthetic MW and MSWI leachates at 20 kPa effective confining stress, whereas the hydraulic conductivity of mock B-P GCLs with 10% linear or crosslinked polymer ranged from 1.5×10^{-9} to 1.4×10^{-7} m/s. As the effective stress increased, the B-P GCLs branched polymer showed a faster decreasing trend than that of Na-B and B-P GCLs with linear or crosslinked polymer.

1. Introduction

Geosynthetic clay liners (GCLs) are manufactured hydraulic barriers comprising a thin layer (5–10 mm) of sodium bentonite (Na-B) sandwiched between two geotextiles. GCLs have been widely used in composite liner systems in waste containment facilities due to their low permeability, ease of installation, and relatively thin thickness (Shackelford et al., 2000; Bouazza, 2002; Jo et al., 2001, 2005; Kolstad et al., 2004; Bradshaw and Benson, 2014; Scalia IV et al., 2014; Bradshaw et al., 2016; Tian et al., 2016, 2019; Setz et al., 2017; Bouazza et al., 2017; McWatters et al., 2019). The hydraulic performance of GCLs is controlled by the Na-B layer (Koerner 2012). The Na-B in GCLs primarily consists of Na-montmorillonite, which has a large surface area and high cation exchange capacity (Mitchell and Soga, 1993). When hydrated with water or dilute solutions, the Na-B undergoes osmotic swelling, which results in narrow and tortuous pathways for liquid flow. This leads to a low hydraulic conductivity of a GCL ($\leq 10^{-10}$ m/s) (Scalia IV et al., 2014; Tian et al., 2019).

However, leachates from coal combustion products (CCR), mining waste (MW), and municipal solid waste incineration ash (MSWI) may

have high ionic strength ($I > 300$ mM), predominantly polyvalent cations, and/or extreme pH conditions (< 3 or > 12), which can inhibit the osmotic swelling of Na-B and lead to high hydraulic conductivity of Na-B GCL ($> 10^{-10}$ m/s) (Athanasopoulos et al., 2015; Salihoglu et al., 2016; Chen et al., 2018; Tian and Benson, 2018; Zainab and Tian, 2020; Li et al., 2021; Wireko and Abichou, 2021). Therefore, the Na-B GCLs have been modified by blending bentonite with organic molecules or polymer to improve chemical compatibility (Ashmawy et al., 2002; Kolstad et al., 2004; Katsumi et al., 2008; Di Emidio et al., 2015; Scalia IV et al., 2014, 2018; Athanasopoulos et al., 2015; Mazzieri and Emidio, 2015; Tian et al., 2016, 2019; Özhan, 2018; Chen et al., 2019; Prongmanee and Chai, 2019; Li et al., 2021; Norris et al., 2022; Wireko et al., 2022). These polymer-modified GCLs, also known as bentonite-polymer (B-P) GCLs, comprise of bentonite-polymer composites (BPC) or a mixture of polymer and bentonite (e.g., dry mixing, dry sprinkling, and wet mixing) (Scalia IV et al., 2014, 2018; Di Emidio et al., 2015; Tian et al., 2016, 2017, 2019; Chen et al., 2019; Zainab et al., 2021; Li et al., 2021; Norris et al., 2022). Polymers used in B-P GCLs include anionic polymers such as sodium carboxymethylcellulose (CMC) (e.g., Di Emidio et al., 2015; Norris et al., 2022) and poly (acrylic acid) (PA) (e.g., Scalia

* Corresponding author.

E-mail address: ktian@gmu.edu (K. Tian).<https://doi.org/10.1016/j.geotexmem.2024.05.006>

Received 20 May 2023; Received in revised form 20 April 2024; Accepted 13 May 2024

Available online 24 May 2024

0266-1144/© 2024 Elsevier Ltd. All rights reserved, including those for text and data mining, AI training, and similar technologies.

IV et al., 2018; Chen et al., 2019; Prongmanee and Chai 2019; Tian et al., 2019; Li et al., 2021; Norris et al., 2022).

Hydraulic conductivity of B–P GCLs permeated with leachates from solid waste disposal facilities such as CCR leachates, MW leachates, and MSWI leachates were investigated and reported in previous literature (Athanasopoulos et al., 2015; Salihoglu et al., 2016; Donovan et al., 2017; Tian and Benson, 2018; Chen et al., 2019; Tian et al., 2019; Zainab et al., 2021; Li et al., 2021; Wireko et al., 2022). In a study conducted by Chen et al. (2019), B–P GCLs with polymer loading >1.9% can significantly improve chemical compatibility compared to Na–B GCLs to CCR leachates. In a study conducted by Li et al. (2021), B–P GCLs with polymer loading >7.5% were shown to maintain a low hydraulic conductivity to hyperalkaline bauxite liquors from Chinese red muds (pH > 12, I = 77–620 mM). The low hydraulic conductivity of B–P GCLs is attributed to the polymer hydrogel clogging mechanism (Tian et al., 2016; 2019; Zainab et al., 2021; Norris et al., 2022). However, the addition of different types of polymers to B–P GCLs may cause different types of clogging mechanisms (Zainab et al., 2021; Chen et al., 2023a). Zainab et al. (2021) concluded that linear polymers create a glue-like substance that binds bentonite particles and crosslinked polymers form small three-dimensional hydrogels that clog the pore spaces between bentonite particles. Chen et al. (2023a, 2023b) concluded that different polymer types might have different characteristics (e.g., tortuosity and roughness) in B–P GCLs permeated with bauxite liquor leachates (I = 622.5 mM), leading to a low hydraulic conductivity. However, limited studies focus on the hydraulic conductivity of B–P GCLs with branched polymer, i.e., linear polymer with side chains.

The objective of this study was to evaluate the hydraulic conductivity of B–P GCLs with three different polymer additives (e.g., branched, linear, and crosslinked) to aggressive CCR, MSWI, and MW leachates. The polymer loadings of the B–P GCLs tested ranged from 3 to 15%. Hydraulic conductivity tests were conducted on mock GCLs with three synthetic leachates at an effective stress of 20 kPa. After chemical and hydraulic equilibrium were reached, the effective confining stress was increased to 100, 250, and 500 kPa to mimic the stresses induced by waste mass placed in a landfill. As a control, comparable hydraulic conductivity tests were also performed on Na–B GCLs. This study investigated the relationship between hydraulic conductivity of B–P GCLs and (1) polymer type (e.g., branched, linear, crosslinked), (2) polymer mass loading, (3) chemical composition of permeant liquid, and (4) the effect of confining stress on B–P GCLs.

2. Materials and methods

2.1. Polymers used in this study

Three proprietary anionic polymers (e.g., branched, linear, and crosslinked) were evaluated in this study, named as polymer A, B, and C, respectively (Table 1). Polymer A is a branched polymer that can be visualized as a linear polymer with side chains of the same polymer

Table 1
Properties of polymers used in this study.

Polymer	Charge ^a	Structure ^a	LOI (%)	Viscosity ^b (mPa.s)	SI ^c (mL/ 2 g)
Polymer A	Anionic	Branched	82.01 ± 0.72	144.2	600
Polymer B	Anionic	Linear	78.69 ± 0.82	96.2	120
Polymer C	Anionic	Crosslinked	96.97 ± 2.29	14.0	140

^a Reported by the manufacturer.

^b The viscosity of polymers was measured in DI water with concentration of 3000 ppm (shear rate = 200 rpm).

^c The swell index tests of polymer were conducted using 0.2 g of oven dried specimens and projected to mL/2 g.

attached to the main chain (McKee, 2017), as shown in Fig. 1. Polymer B is a linear polymer, in which monomeric units with hydrophilic functional groups are covalently linked together to form the polymer chain (Chatterji and Borchardt, 1981). The linear (and linear branched) polymer can disperse and swell in the solution to form a viscous polymer gel, which are referred to as water-soluble polymers (Williams, 2007; Rivas et al., 2018). Polymer C is a crosslinked polymer, which is a result of bonding polymer chains through crosslinking. The crosslinked polymers can swell in solutions to hold a large amount of water when hydrated to form discrete polymer hydrogels. Polymers A and C were finer than polymer B. More than 75% of polymers A and C passed the #100 sieve, and only a small portion of polymer B passed the #100 sieve (Fig. 1 and Fig. A1).

The initial loss on ignition (LOI) of the three polymers ranged from 78.67% to 96.97% (ASTM D7348). The swell index of polymer A in DI water was approximately five times higher than that of polymer B and Polymer C (e.g., 600 mL/2 g vs. 120–140 mL/2 g). The viscosity of the polymers was measured in DI water following ASTM D2196. The tested polymer concentration was 3000 ppm, and the shear rate was controlled at 200 rpm (Gao, 2013; Geng et al., 2016, 2022; Devrani et al., 2017). The viscosity of polymer A was slightly higher than polymer B (144.2 mPa.s vs. 96.2 mPa.s), and the viscosity of polymer C was the lowest (e.g., 14 mPa.s). This result indicates that polymer A and B showed strong interaction between the polymer and water molecules and extensions of the polymer chains, which results in greater shear resistance and a corresponding higher viscosity. The linear polymers undergo a central scission in strong flow due to buildup of stress from fluid drag, whereas the branched polymer showed higher shear stability against such scission with a corresponding higher viscosity value (Xue et al., 2005).

2.2. B–P GCL

B–P composites were created by dry mixing Na–B and polymer (Norris et al., 2022). The calculated quantity of dry bentonite was dry mixed with each polymer and then tumbled at 50 rpm for a minimum of 24 h to allow uniform mixing. The polymer loading in GCLs used in this study ranged from 3% to 15%. B–P composite was spread uniformly on the carrier non-woven geotextiles, and then another non-woven geotextile was placed on the top to create a mock GCL. The mass per unit area of the mock GCLs was 4.0 kg/m². The B–P GCLs were named B–P-A-3, B–P-B-3, B–P-A-5, B–P-B-5, B–P-C-5, B–P-A-10, B–P-B-10, B–P-C-10, and B–P-A-15. The capital letters “A, B, and C” indicate the polymer type, and the numeric digits indicate the polymer loading of the B–P GCLs.

2.3. Permeant solutions

The permeant solution was characterized based on the ionic strength (I), relative abundance of monovalent and polyvalent cations (RMD), and pH. Ionic strength is defined as:

$$I = \frac{1}{2} \sum_{i=1}^n C_i Z_i^2 \quad (1)$$

where C_i = molar concentration of i th ion in solution; and Z_i = valence of the i th ion.

Kolstad et al. (2004) quantified the RMD in permeant leachate:

$$RMD = \frac{M_M}{\sqrt{M_D}} \quad (2)$$

where M_M = total molarity of monovalent cations; and M_D = total molarity of divalent cations.

Fig. 2 shows the relationship between ionic strength and RMD of the CCR, MSWI, and MW leachates compiled from literature (Ashmawy et al., 2002; Abdelaal et al., 2011; Athanasopoulos et al., 2015; Townsend et al., 2015; Ghazizadeh et al., 2018; Tian and Benson, 2018;

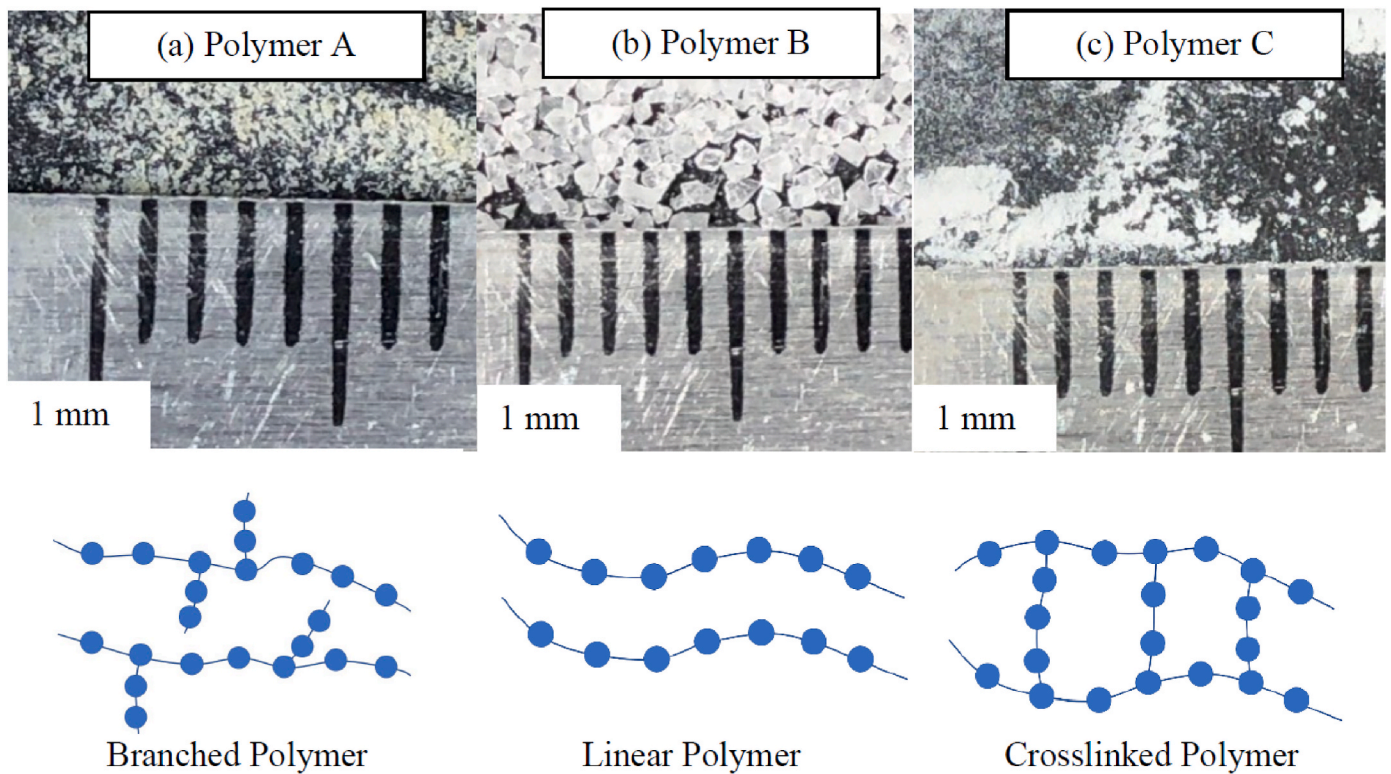


Fig. 1. Images of polymer used in this study (a) polymer A, (b) polymer B, (c) polymer C.

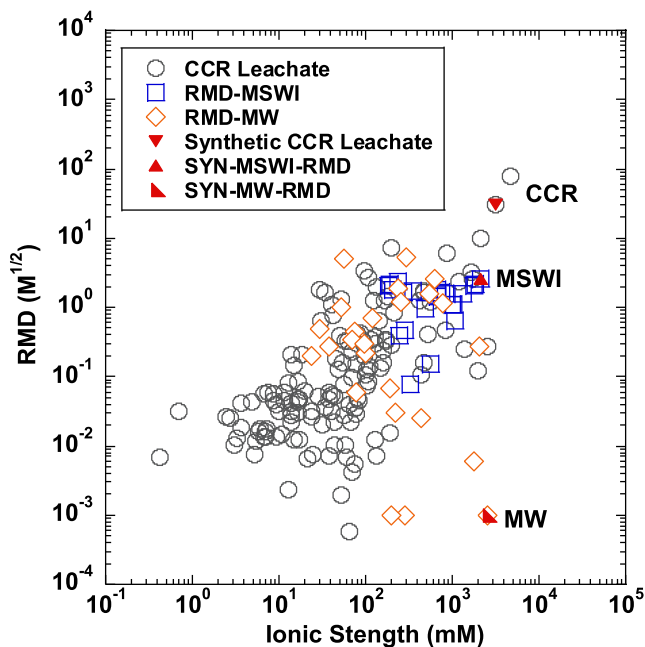


Fig. 2. Ionic strength versus RMD of CCR, MSWI, and MW leachates in literature, along with the synthetic leachates in this study. (Note: Data from literature was obtained from Ashmawy et al. (2002); Abdelaal et al. (2011); Athanassopoulos et al. (2015); Townsend et al. (2015); Ghazizadeh et al. (2018); Tian and Benson (2018); Zainab et al. (2021); Li et al. (2021); Wireko et al. (2022)).

Zainab et al., 2021; Li et al., 2021; Wireko et al., 2022).

The CCR leachate data was collected from 130 disposal sites located within the United States. The ionic strength of CCR leachates ranged

from 0.42 mM to 4685 mM, and the RMD ranged from a minimum value of $0.002 \text{ M}^{1/2}$ to a maximum of infinity (leachate samples without divalent cations) (Zainab et al., 2021). Synthetic CCR leachate in this study was selected to represent a leachate with high ionic strength ($I = 3179 \text{ mM}$, $\text{RMD} = 32.0 \text{ M}^{1/2}$), as reported in Zainab et al. (2021) and Li et al. (2021). MW leachates include gold, copper, and bauxite mining leachates (Ghazizadeh et al., 2018). The bauxite mining leachate contains elevated concentrations of aluminum (Al) and sodium (Na), with high pH (>12 in some cases) (Tian and Benson, 2018; Li et al., 2021). The copper mining leachates were more aggressive than bauxite mining leachates, with ionic strength up to 2580 mM and pH of 2.0 (Ghazizadeh et al., 2018). The synthetic MW leachates were representative of copper mine-process leachates with low pH = 2.0 and high ionic strength ($I = 2580 \text{ mM}$, $\text{RMD} = 0.012 \text{ M}^{1/2}$) as reported by Abdelaal et al. (2011). The MSWI leachates are representative of landfills, where incineration ash is either disposed alone in an ash mono-fill or co-disposed with regular MSW in the United States (Wireko et al., 2022). The ionic strength of MSWI leachates ranged from 182 to 2128 mM, and RMD ranged from 0.077 to $2.63 \text{ M}^{1/2}$, reported by Ashmawy et al. (2002), Townsend et al. (2015), and Wireko et al. (2022). The synthetic MSWI leachates were representative of leachates from an ash mono-fills with the highest ionic strength ($I = 2128 \text{ mM}$, $\text{RMD} = 2.62 \text{ M}^{1/2}$) (Townsend et al., 2015). The concentration of major cations, anions, and the bulk properties (I , RMD, and pH) of synthetic leachates selected are given in Table 2. All the synthetic leachates were prepared by dissolving reagent-grade NaCl, KCl, $\text{CaCl}_2 \cdot 2\text{H}_2\text{O}$, $\text{MgCl}_2 \cdot 6\text{H}_2\text{O}$, MgSO_4 , and K_2SO_4 in Type II DI water per ASTM D1193. The synthetic MW leachate was titrated with HCl solution to adjust to the target pH.

2.4. Hydraulic conductivity test

Hydraulic conductivity tests were conducted on 152.4 mm (6-inch) circular GCL specimens in flexible wall permeameters using the falling headwater and constant tailwater method in accordance with ASTM D6766. All the mock GCL specimens were first hydrated in the

Table 2
Properties of synthetic leachates.

Leachate	Ionic strength	RMD (M ^{1/2})	Major cations (M)				Major anions (M)		pH	EC (mS/cm)
	(M)		Na ⁺	K ⁺	Mg ²⁺	Ca ²⁺	Cl ⁻	SO ₄ ²⁻		
CCR	3.18	30.54	2.28	0.02	–	–	0.59	0.86	8.2	86.8
MSWI	2.13	2.63	1.34	–	0.03	0.23	1.87	0.00	8.0	75.9
MW	2.58	0.01	–	–	0.64	0.01	0.13	0.60	2.0	50.3

permeameter with the specific leachate at an effective confining stress of 20 kPa for 48 h with a hydraulic head of 1.30 m. Effluent was collected in 70 mL polyethylene bottles and effluent pH and EC were periodically measured. The tests were continued until hydraulic and chemical equilibrium were achieved in accordance with ASTM D6766. Once both the chemical and hydraulic equilibrium were reached, the effective confining stress was increased to 100, 250, and 500 kPa to mimic the stresses induced by waste mass placed in a landfill.

2.5. Swell index test

The swell index (SI) of mock Na–B and B–P GCLs was measured using DI water and synthetic leachates in accordance with ASTM D5890. The SI was measured as the volume of the swollen specimen in a graduated cylinder after 24 h (in mL/2 g). To avoid possible loss of polymer mass during sieving processes, the B–P composite was prepared by mixing dry polymer with Na–B that passed the #200 sieve (Wireko et al., 2020). SI tests of polymers were conducted using 0.2 g of oven dried specimens which were added to an empty 100 mL graduated cylinder. Leachate was gradually added in increments of 1 mL every 10 min. The tests were performed until no swelling was observed after adding the water and the SI (mL/0.2 g) was then recorded as the final volume of the swollen specimen. The swell index of polymer was then projected to mL/2 g (Wireko et al., 2020).

2.6. Viscosity test

The viscosity of a B–P slurry is indicative of polymer-bentonite interaction when the B–P is hydrated with a specific solution and can reflect the chemical compatibility of B–P GCLs (Geng et al., 2016, 2022). Viscosity tests were conducted following a procedure outlined by Geng et al. (2022) and Vryzas et al. (2017). The B–P and Na–B suspensions were prepared by gradually adding 15 g of air-dried B–P composite or Na–B (in increments of 1 g) to a beaker already filled with 300 mL of corresponding solution (solid-liquid ratio = 5%) and stirred using a magnetic bar stirrer at approximately 720 rpm for more than 180 min. The beakers were covered with Parafilm and hydrated for 24 h. The suspensions were then stirred using a magnetic bar for no less than 120 min prior to conducting the viscosity tests. The viscosity of the suspensions was measured using a ViscoQC 100. Spindle type and rotational speed were selected so the viscosity reading fell within 10–90% torque as recommended.

2.7. LOI test

Loss on ignition (LOI) tests are commonly used to determine the polymer content of B–P GCLs (Scalia IV et al., 2014; Tian et al., 2016; Gustitus et al., 2021; Li et al., 2021). LOI tests were conducted with pure polymer, Na–B, and B–P composite. The known mass of pure polymer, Na–B, and B–P composite specimens were ground to pass a No. 20 woven wire sieve (ASTM E11; ASTM 2013) and dried for 24 h in the oven at 105 °C to remove moisture in the test specimens. 3 g of oven-dried specimens were placed in a furnace at 550 °C for 4 h, which exceeds the decomposition temperature of polyacrylate (≈ 200 °C). After, the specimens were removed from the furnace and allowed to cool in a water-free atmosphere, the samples were weighed using a microbalance with an accuracy of 0.1 mg (ASTM D7348).

With the measured component (e.g., Na–B and pure polymer) and the B–P composite LOI values, the polymer loading of B–P composite was determined by discounting the LOI of Na–B from the LOI of polymer. Residual polymer loading of B–P GCLs (i.e. polymer loading after conclusion of the hydraulic conductivity tests) were determined using a similar procedure. The Na–B and B–P composites were extracted from three spots on mock GCL samples after the termination of the hydraulic conductivity tests. The residual polymer loading of B–P GCL samples was calculated based on the LOI of Na–B GCL samples that were permeated with the same leachates, because the LOI of Na–B after permeation may differ compared to the LOI of fresh Na–B due to the cation exchange process (Gustitus et al., 2021).

3. Results and discussions

3.1. Swell index

The swell index test results of Na–B, pure polymer, and B–P composite in DI water, synthetic MSWI, MW, and CCR leachates are shown in Fig. 3. The swell index of Na–B to DI water was 28 mL/2 g and decreased to 2.0–3.5 mL/2 g when hydrated in synthetic MSWI, MW, and CCR leachates, where only crystalline swelling occurs (Norris and Quirk 1954; Jo et al., 2001). The B–P composite had a higher swell index than that of Na–B when exposed to the same leachate due to the high swelling of the polymer hydrogel. This result is consistent with conclusions reported by Chen et al. (2019) and Zainab et al. (2021). The swelling of all three polymers in DI water ranged from 120–600 mL/2 g and decreased to 50–260 mL/2 g in synthetic leachates (Fig. 3b), which were much higher than that of Na–B at the same testing conditions. However, the swelling of polymer hydrogels was also suppressed in synthetic leachates due to the high ionic strength and low pH (e.g., MW leachate). As a result, the swelling of B–P composite specimens ranged from 5 to 14 mL/2 g in synthetic leachates, and the swelling of B–P composite specimens gradually increased as the polymer loading increased.

3.2. Hydraulic conductivity

A summary of the hydraulic conductivity tests performed on the Na–B and B–P GCLs using the synthetic leachates is shown in Table 3. Test durations were up to 477 days. All mock Na–B and B–P GCL specimens permeated with synthetic leachates achieved both hydraulic and chemical equilibrium.

The hydraulic conductivity of Na–B and B–P GCLs to synthetic CCR, MSWI, and MW leachates as a function of initial polymer loading is shown in Fig. 4. A higher hydraulic conductivity was measured for Na–B GCL permeated with CCR leachate as shown in Fig. 4a (e.g., 7.1×10^{-7} m/s). The B–P GCLs (e.g., B–P-A, B–P-B, and B–P-C) with 3% or 5% polymer loading had higher hydraulic conductivity (e.g., ranging from 4.6×10^{-7} m/s to 1.1×10^{-7} m/s), which showed a similar hydraulic conductivity to Na–B GCLs permeated with CCR leachate. This result is consistent with Zainab et al. (2021), who reported that B–P GCLs with polymer loading < 5% cannot maintain a low hydraulic conductivity ($< 1 \times 10^{-10}$ m/s) to leachate with CCR aggressive leachates ($I > 473$ mM). As the polymer loading increased to 10%, the hydraulic conductivity of B–P-A and B–P-C GCLs decreased by two orders of magnitude, ranging from 1.2×10^{-9} m/s to 1.5×10^{-9} m/s, whereas mock B–P-B-10 GCL still showed similar hydraulic conductivity with that of the Na–B GCLs

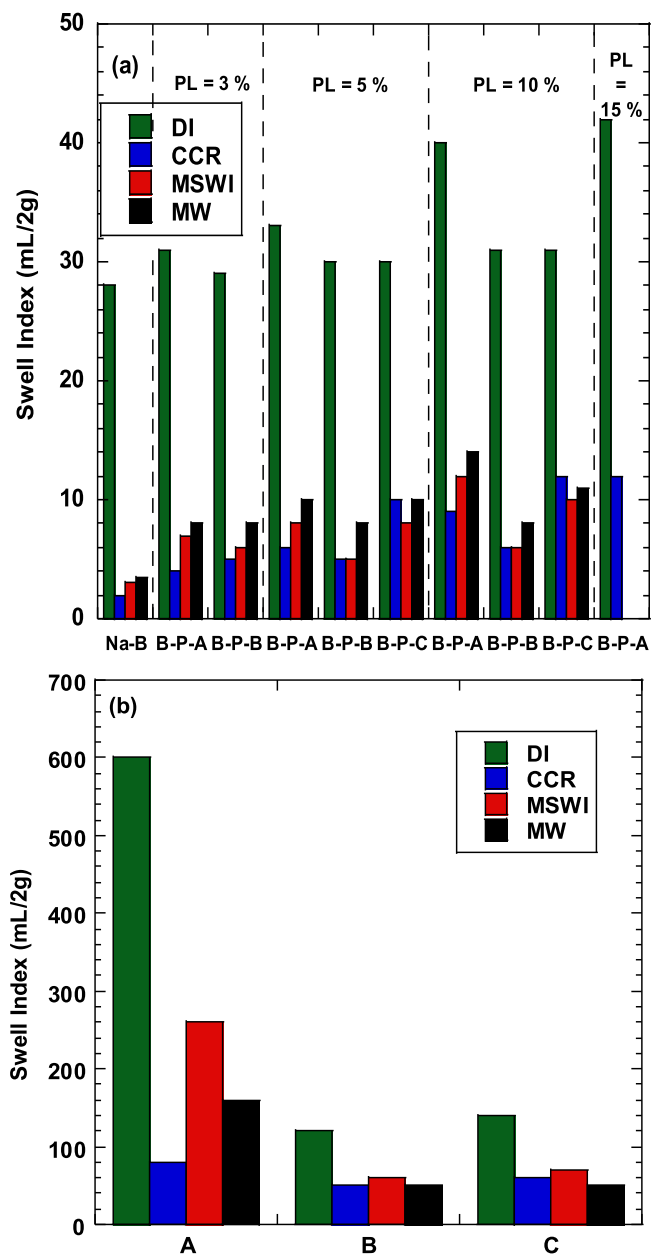


Fig. 3. Swell index of (a) Na-B and B-P composite, (b) pure polymer in CCR, MSWI and MW leachates.

(1.4×10^{-7} vs. 7.1×10^{-7} m/s). When the polymer loading was increased to 15%, the B-P-A GCL maintained lower hydraulic conductivity to CCR leachate (e.g., 1.1×10^{-11} m/s).

Test results of Na-B and B-P GCLs to MSWI leachate are shown in Fig. 4b. The hydraulic conductivity of Na-B GCL was 6.7×10^{-7} m/s. The hydraulic conductivity of B-P-B and B-P-C GCLs, with 3 and 5% polymer loading, to MSWI leachate, was slightly lower than that of Na-B GCLs (e.g., 2.1×10^{-7} – 5.8×10^{-7} vs. 6.7×10^{-7} m/s), whereas the hydraulic conductivity of B-P-A-3 and B-P-A-5 GCLs were approximately two orders of magnitude lower than that of the Na-B GCL (e.g., 4.3×10^{-9} – 1.1×10^{-8} vs. 6.7×10^{-7} m/s). As the polymer loading increased to 10%, both B-P-B-10 and B-P-C-10 GCLs still showed higher hydraulic conductivities to MSWI leachate (e.g., 1.9×10^{-8} to 1.2×10^{-7} m/s). In contrast, B-P-A-10 GCL maintained a low hydraulic conductivity to MSWI leachate (e.g., 8.9×10^{-12} to 1.4×10^{-11} m/s).

Hydraulic conductivity tests conducted with MW leachate had a

similar trend to tests conducted with CCR and MSWI leachates (Fig. 4c). B-P-B and B-P-C with 3%, 5%, and 10% polymer loading had higher hydraulic conductivities to MW leachate, ranging from 4.2×10^{-7} to 8.6×10^{-8} m/s, which were approximately 1.2–8.8 times lower than that of Na-B GCL at the same testing condition. In contrast, B-P-A-5 GCL showed much higher chemical compatibility than B-P-B and B-P-C GCLs, i.e., the hydraulic conductivity of B-P-A-5 GCL was slightly higher than 1×10^{-10} m/s, which is two orders of magnitude lower than that of the B-P-B-5 and B-P-C-5 GCLs. As the polymer loading increased to 10%, only B-P-A-10 GCLs maintained a lower hydraulic conductivity to MW leachate (e.g., 1.0×10^{-11} – 7.5×10^{-11} m/s).

3.3. Hydraulic conductivity vs. swell index

The relationship between swell index and hydraulic conductivity of Na-B and B-P GCLs is shown in Fig. 5. The Na-B GCLs showed higher hydraulic conductivity (e.g., 4.9×10^{-7} to 7.1×10^{-7} m/s) due to low swell index (2.0–3.5 mL/2 g) when permeated with all three synthetic leachates. This result is consistent with conclusions reported by Chen et al. (2019) and Tian et al. (2019). The hydraulic conductivity of B-P GCLs decreased from 5.8×10^{-7} to 8.9×10^{-12} m/s as the swell index increased from 5 to 14 mL/2 g. However, decoupling behavior between the swell and hydraulic conductivity was also observed for B-P GCLs. For example, the hydraulic conductivity of B-P GCL ranged from 1.3×10^{-10} m/s (e.g., B-P-A) to 3.2×10^{-7} m/s (e.g., B-P-C) with a swell index around 10 mL/2 g. Additionally, both lower hydraulic conductivity ($< 10^{-10}$ m/s) and higher hydraulic conductivity ($> 10^{-10}$ m/s) of B-P GCLs were shown at a similar swell index (e.g., 12 mL/2 g). These results agree with previous studies that both swelling and polymer clogging mechanisms control the hydraulic conductivity of B-P GCLs (Scalia IV et al., 2014, 2018; Tian et al., 2016, 2019; Zainab et al., 2021; Li et al., 2021; Norris et al., 2022). In comparison with B-P-B and B-P-C GCLs, the B-P-A GCL showed a faster decreasing trend in hydraulic conductivity as the swell index increased. For example, the hydraulic conductivity of B-P-A GCLs decreased to 10^{-11} m/s, as the swell index increased to 12 mL/2 g, whereas B-P-C GCLs maintained higher hydraulic conductivity (e.g., 10^{-9} m/s) with a swell index of 12 mL/2 g. This observation illustrates that the B-P-A GCL has higher chemical compatibility than that of B-P-B and B-P-C GCLs at the same polymer loading. This indicates that the type of polymer hydrogel affects the chemical compatibility of B-P GCLs.

3.4. Viscosity

The viscosity of Na-B and B-P composite suspensions in synthetic leachates is shown in Fig. 6. The viscosity of Na-B suspensions ranged from 7.5 to 8.0 mPa.s, whereas the viscosity of B-P composite suspensions ranged from 10.3 to 38.2 mPa.s. The higher viscosity of B-P GCL was attributed to the bonding between the polymer and water molecules (Geng et al., 2016). Also, adding polymer may lead to more effective bridging (i.e., due to attraction between polymer and bentonite particles) among the bentonite particles, and voids between the bentonite particles were closed which resulted in more shear resistance (Guler et al., 2018). For B-P GCLs with the same polymer type, with the increase of the polymer loading, the viscosity of B-P composite to same leachate also increased. For example, the viscosity of B-P-B-5 composite was 17.5 mPa.s when hydrated with CCR leachate, whereas the B-P-B-10 showed higher viscosity to CCR leachate (e.g., 26.6 mPa.s). This can be explained by the presence of more polymer chains and more intensive hydrogel formation (Geng et al., 2016). In addition, the viscosity of B-P-A composite was similar to the B-P-B composite but higher than the B-P-C composite when exposed to the same leachates. The difference in viscosity is attributed to the different polymer types among the B-P-A, B-P-B, and B-P-C composites. Crosslinked polymer (Polymer C) takes part in hydrogel swelling, lacks entanglement among the bentonite particles and slightly extends to the viscosity of the bentonite

Table 3
Hydraulic conductivity of GCLs permeated with synthetic leachates.

GCL	Permeant liquid	PVF	Total test Time (days)	Termination criteria		Hydraulic conductivity (m/s)			
				Hydraulic equilibrium	Chemical equilibrium	20 kPa	100 kPa	250 kPa	500 kPa
Na-B	CCR	32.6	42	Yes	Yes	7.1×10^{-7}	2.9×10^{-7}	1.6×10^{-7}	6.2×10^{-8}
	MSWI	40.2	59	Yes	Yes	6.7×10^{-7}	4.4×10^{-7}	9.7×10^{-8}	7.8×10^{-9}
	MW	36.7	61	Yes	Yes	4.9×10^{-7}	5.3×10^{-7}	8.8×10^{-8}	2.4×10^{-8}
B-P-A-3	CCR	32.4	106	Yes	Yes	4.2×10^{-7}	7.8×10^{-10}	8.2×10^{-11}	5.6×10^{-12}
	MSWI	20.5	102	Yes	Yes	1.1×10^{-8}	7.1×10^{-11}	4.9×10^{-11}	4.1×10^{-12}
	MW	25.5	147	Yes	Yes	5.1×10^{-8}	3.5×10^{-11}	2.5×10^{-11}	6.4×10^{-12}
B-P-A-5	CCR	33.7	124	Yes	Yes	1.1×10^{-7}	1.1×10^{-10}	3.4×10^{-11}	3.2×10^{-12}
	MSWI	31.4	144	Yes	Yes	4.3×10^{-9}	3.9×10^{-11}	4.6×10^{-12}	3.4×10^{-12}
	MW	19.5	114	Yes	Yes	1.3×10^{-10}	6.7×10^{-12}	4.2×10^{-12}	2.1×10^{-12}
B-P-A-10	CCR	38.5	148	Yes	Yes	1.2×10^{-9}	5.3×10^{-11}	8.1×10^{-12}	4.7×10^{-12}
	MSWI	24.6	138	Yes	Yes	1.4×10^{-11}	4.5×10^{-12}	3.2×10^{-12}	2.2×10^{-12}
	MW	33.3	190	Yes	Yes	7.5×10^{-11}	3.0×10^{-11}	7.0×10^{-12}	4.1×10^{-12}
	MSWI (Duplicate)	39.7	472	Yes	Yes	8.9×10^{-12}			
	MW (Duplicate)	26.2	467	Yes	Yes	1.0×10^{-11}			
B-P-A-15	CCR	74.3	477	Yes	Yes	1.1×10^{-11}			
B-P-B-3	CCR	36.5	48	Yes	Yes	4.6×10^{-7}	8.3×10^{-8}	7.6×10^{-9}	4.3×10^{-10}
	MSWI	38.7	51	Yes	Yes	4.1×10^{-7}	1.5×10^{-8}	1.3×10^{-9}	8.6×10^{-10}
	MW	35.5	47	Yes	Yes	4.2×10^{-7}	5.0×10^{-8}	6.2×10^{-9}	5.4×10^{-9}
B-P-B-5	CCR	31.2	55	Yes	Yes	3.1×10^{-7}	1.5×10^{-8}	1.2×10^{-9}	1.6×10^{-10}
	MSWI	35.5	47	Yes	Yes	2.1×10^{-7}	2.1×10^{-8}	3.9×10^{-9}	1.4×10^{-10}
	MW	29.2	112	Yes	Yes	3.2×10^{-7}	5.1×10^{-9}	3.8×10^{-10}	5.1×10^{-11}
B-P-B-10	CCR	28.8	92	Yes	Yes	1.4×10^{-7}	4.4×10^{-8}	2.5×10^{-10}	5.0×10^{-12}
	MSWI	29.9	97	Yes	Yes	1.2×10^{-7}	4.8×10^{-9}	5.4×10^{-10}	4.4×10^{-12}
	MW	34.1	114	Yes	Yes	1.0×10^{-7}	1.1×10^{-8}	2.7×10^{-11}	2.9×10^{-12}
B-P-C-5	CCR	29.6	63	Yes	Yes	4.2×10^{-7}	8.6×10^{-9}	2.7×10^{-9}	7.5×10^{-10}
	MSWI	32.2	57	Yes	Yes	5.8×10^{-7}	4.2×10^{-8}	1.5×10^{-8}	1.7×10^{-10}
	MW	34.8	84	Yes	Yes	8.6×10^{-8}	1.6×10^{-8}	5.7×10^{-9}	1.4×10^{-10}
B-P-C-10	CCR	31.4	114	Yes	Yes	1.5×10^{-9}	6.1×10^{-11}	8.4×10^{-12}	4.5×10^{-12}
	MSWI	30.8	128	Yes	Yes	1.9×10^{-8}	3.1×10^{-9}	5.6×10^{-11}	7.2×10^{-12}
	MW	29.6	177	Yes	Yes	5.6×10^{-8}	2.8×10^{-8}	2.0×10^{-9}	1.2×10^{-11}

suspension. The viscosity of polymer A (branched polymers) was higher than that of polymer B (linear polymers) (144.2 vs. 96.2 mPa.s in DI water). Caminade et al. (2019) and Zhang et al. (2013) reported that linear-branched architectures are more favorable for the interaction with clays compared with the linear polymers due to branched polymers having a better ability to catch smaller bentonite particles than that of linear polymers.

The relationship between viscosity and hydraulic conductivity of Na-B and B-P GCLs is shown in Fig. 7. The Na-B GCLs showed high hydraulic conductivity to all three leachates (e.g., 4.9×10^{-7} to 7.1×10^{-7} m/s) with low viscosity (e.g., < 8.0 mPa.s). The hydraulic conductivity of B-P-B GCLs were also higher than 10^{-10} m/s with the viscosity ranging from 9.7 to 28.0 mPa.s, whereas the hydraulic conductivity of B-P-A GCLs decreased from 4.2×10^{-7} to 1.1×10^{-11} m/s as the viscosity increased from 18.9 to 32.1 mPa.s. This indicates that entanglement between polymer and bentonite in B-P-A GCLs were better than B-P-B GCLs, which resulted in higher viscosity in the pore fluid and lower hydraulic conductivity. The high viscosity of B-P-A suspension (e.g., B-P-A-10 to MSWI and MW leachates, and B-P-A-15 to CCR leachate) was associated with well-developed polymer hydrogel and more effective polymer bentonite entanglement (Caminade et al., 2019), which resulted in narrower pore space and lower hydraulic conductivity.

3.5. Polymer elution

The comparison of initial and residual polymer loading of mock B-P-A, B-P-B, and B-P-C GCLs to CCR, MSWI, and MW leachates is shown in Fig. 8. The residual polymer loading of all B-P GCLs was lower than the initial polymer loading, which indicates that polymer was eluted from all three polymer types of B-P GCLs during permeation. The polymer eluted more from mock B-P-B than that of mock B-P-A GCLs when permeated with the same leachate. The polymer loading of B-P-A-10 GCLs decreased from 10.0% to 7.5% when permeated with MW leachate, whereas the polymer loading of mock B-P-B-10 decreased

from 10.0% to 5.8%. The results indicate that increasing the number of branches on the polymer chain decreased the disparity in the lengths of the surfactants and a polymeric arm, thus promoting entanglement between the polymer and clay (Singh and Balazs 2000). As a result, the polymer elution from B-P-A was much less than that of B-P-B at the same testing condition, as shown in Fig. 8. In contrast, the polymer eluted from B-P-C-10 GCL decreased from 10.0% to 5.5% when permeated with MW leachate. The 3D polymer hydrogel is mainly mechanically entrapped in bentonite, leading to clogging of the pore spaces within the bentonite, resulting in a low hydraulic conductivity (Scalia IV et al., 2014; Tian et al., 2019; Zainab et al., 2021). However, the 3D polymer hydrogel could be highly inhibited due to very aggressive leachate ($I > 2000$ mM) (Tian et al., 2019). Therefore, substantial inhibited 3D polymer hydrogel can be eluted from the large intergranular pores (Tian et al., 2019). Chen et al. (2023a) also concluded that polymer type affects the polymer elution of B-P GCLs during the hydraulic conductivity tests and can change other characteristics, such as tortuosity and roughness.

The relationship between the hydraulic conductivity of B-P GCLs and residual polymer loading is shown in Fig. 9. The initial polymer loadings of the B-P GCLs tested ranged from 3 to 15 %. All B-P tests showed high hydraulic conductivity (e.g., higher than 10^{-10} m/s) to synthetic leachates with residual polymer loading lower than 6.0%. In contrast, only B-P-A GCLs with a residual polymer loading higher than 7.0% can maintain a low hydraulic conductivity to synthetic MSWI and MW leachates. The results show that polymer retention is critical to maintain the low hydraulic conductivity of B-P GCLs.

3.6. Effect of effective stress

Hydraulic tests were conducted with B-P GCLs to synthetic leachates at elevated confining stress to mimic the stress induced during land-filling. Temporal behavior of the mock B-P-A-5 GCL permeated with CCR leachate is shown in Fig. 10. Hydraulic equilibrium was achieved at the early stage of the test where the Q_{out}/Q_{in} was within $1 \pm 25\%$

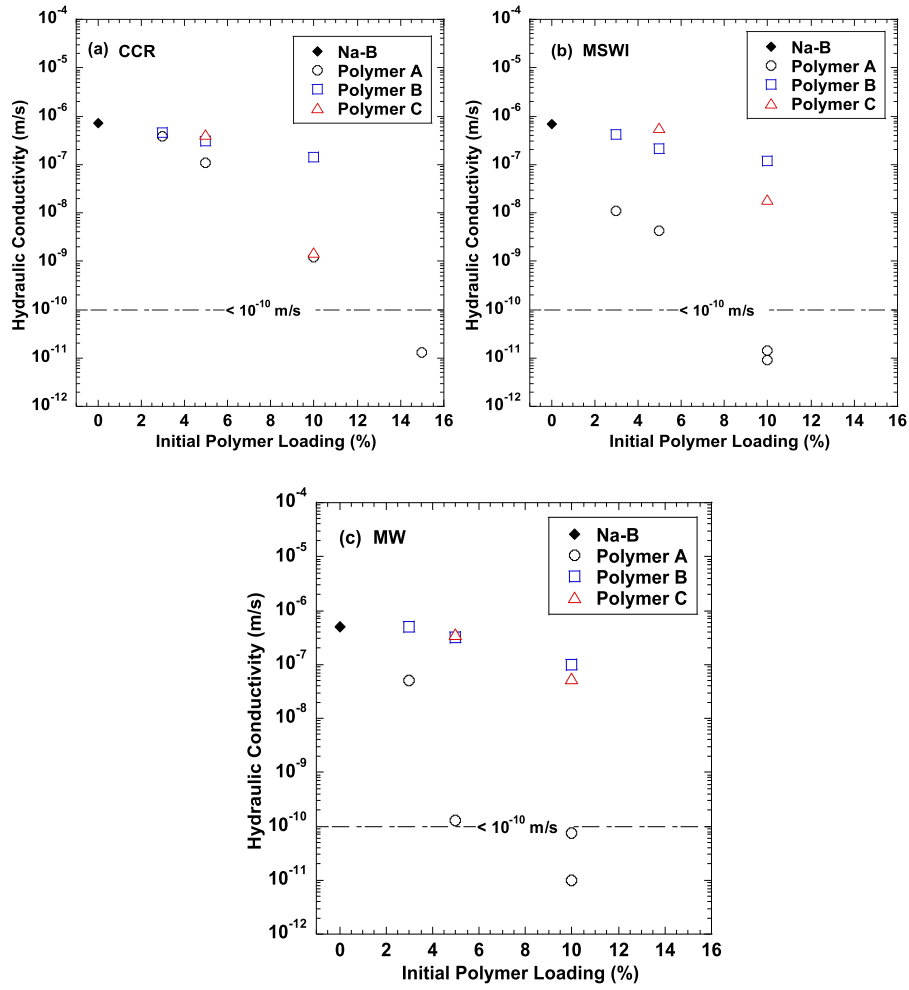


Fig. 4. Hydraulic conductivity of mock GCLs to synthetic leachates as a function of initial polymer loading at 20 kPa, (a) to CCR leachate; (b) to MSWI leachate; (c) to MW leachate.

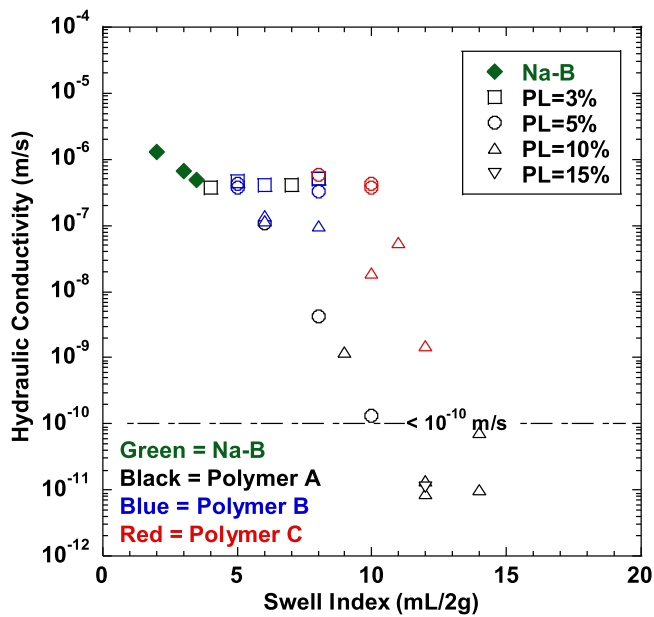


Fig. 5. Hydraulic conductivity of mock Na-B and B-P GCLs to synthetic leachates as a function of swell index.

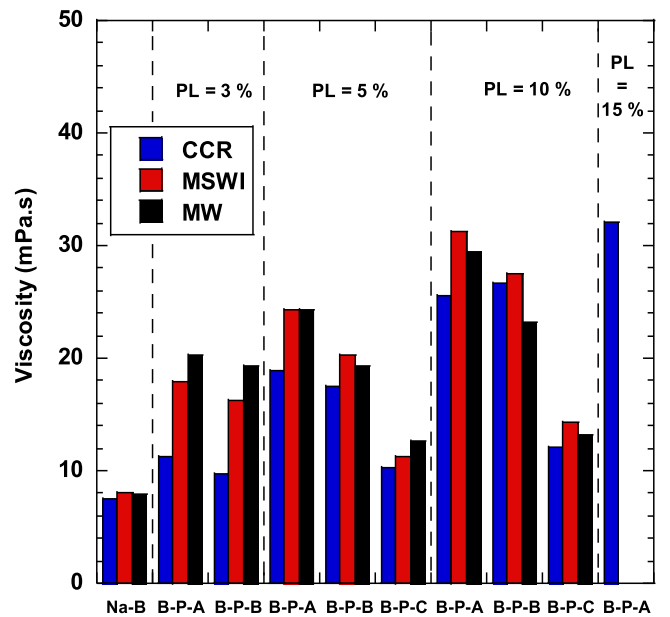


Fig. 6. Viscosity of Na-B and B-P suspensions in synthetic leachates.

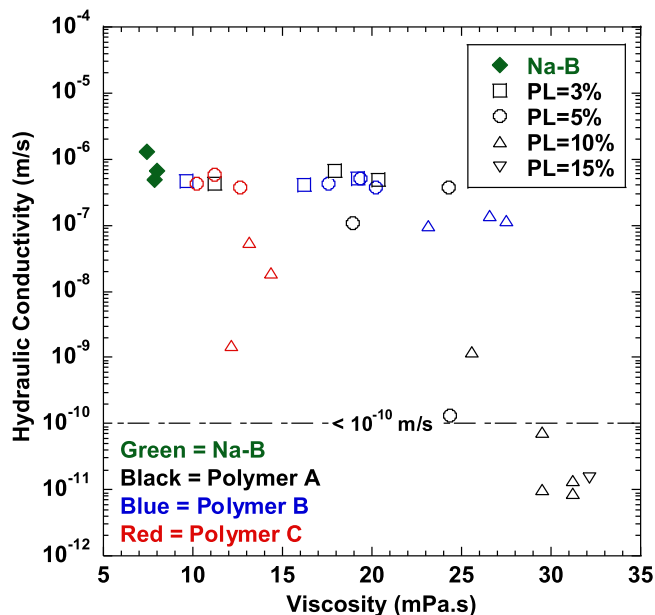


Fig. 7. Hydraulic conductivity of mock Na-B and B-P GCLs to synthetic leachates versus viscosity.

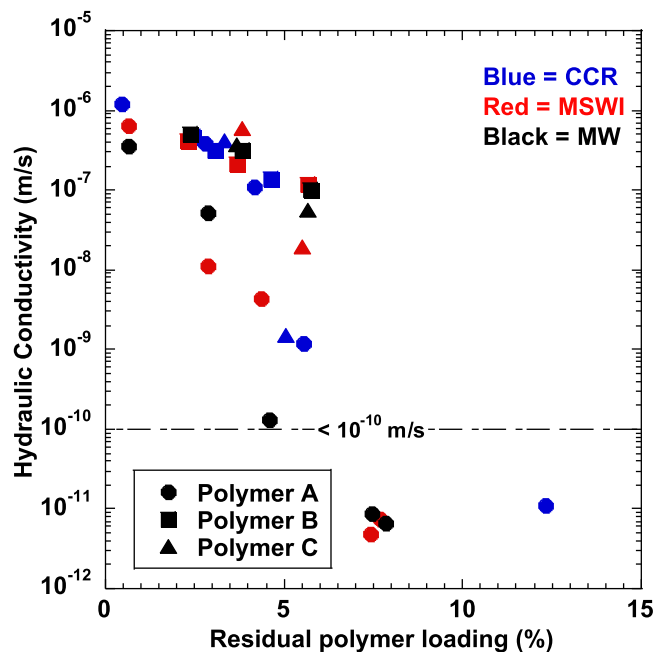


Fig. 9. Hydraulic conductivity of B-P GCLs to synthetic leachates as a function of residual polymer loading after permeation.

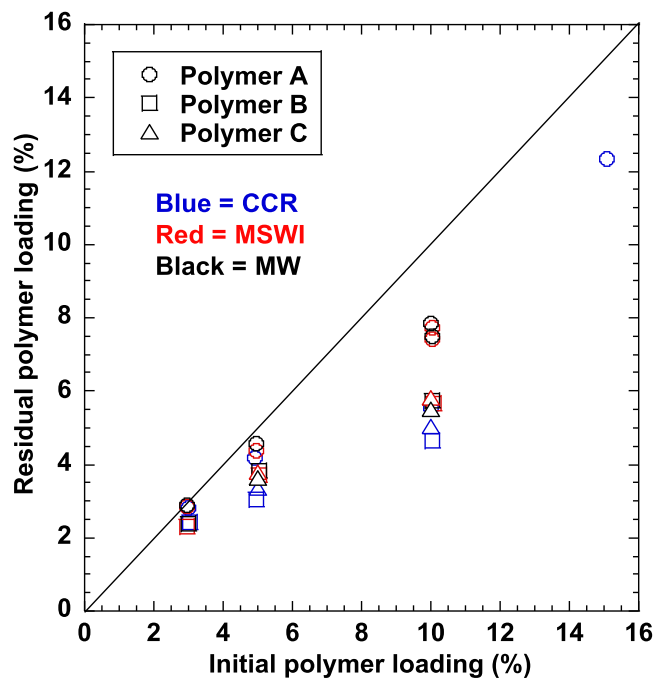


Fig. 8. Comparison between initial and residual polymer loading of mock B-P GCLs after hydraulic conductivity test.

(Fig. 10a). The chemical equilibrium was reached around 12 PVF, i.e., both EC and pH of the effluent leveled off and fell within the $1 \pm 10\%$ of the EC and pH in the influent (Fig. 10b). The effective confining stress was then increased from 20 kPa to 100 kPa, 250 kPa, and 500 kPa. The hydraulic conductivity of mock B-P-A-5 GCL decreased from 1.1×10^{-7} m/s to 1.1×10^{-10} m/s when the confining stress increased from 20 kPa to 100 kPa. At 250 kPa, the hydraulic conductivity of mock B-P-A-5 GCL decreased approximately one order of magnitude (e.g., 3.4×10^{-11} m/s). As the confining stress increased to 500 kPa, the hydraulic conductivity of mock B-P-A-5 GCL further decreased to 3.2×10^{-12} m/s.

A summary of the hydraulic conductivity of B-P GCLs to synthetic leachates at elevated confining stress is shown in Table 3. As the effective stress increased to 500 kPa, the hydraulic conductivity of Na-B and B-P GCLs to synthetic leachate exhibited a decreasing trend. However, the decreasing trends vary depending on polymer loading and polymer type in GCLs. A comparison of the hydraulic conductivity of Na-B and B-P GCLs permeated with synthetic CCR leachate as a function of effective confining stress is shown in Fig. 11. The hydraulic conductivity of Na-B GCLs to synthetic CCR leachate decreased as the effective stress increased from 20 to 500 kPa, but still was higher than 10^{-10} m/s even at 500 kPa. All the B-P GCLs showed a faster decreasing trend than that of Na-B GCLs as the effective confining stress increased. In addition, the hydraulic conductivity of B-P GCLs with higher polymer loading decreased at a faster rate compared to B-P GCLs with the same type of polymer. For example, as the effective stress increased from 20 to 500 kPa, the B-P-B-10 showed low hydraulic conductivity ($< 10^{-10}$ m/s) when permeated with CCR leachate, whereas the hydraulic conductivity of B-P-B-5 was higher than 10^{-10} m/s at 500 kPa. Li et al. (2021) also reported a comparable observation that B-P GCLs with higher polymer loading showed a faster decreasing trend when permeated with CCR leachate as the effective stress increased from 20 kPa to 500 kPa. In addition, this study reveals that the polymer type of B-P GCLs also affects the beneficial effect of increasing effective confining stress in decreasing of hydraulic conductivity of B-P GCLs. The B-P-A GCL (branched polymer) decreased faster than B-P-B (linear polymer) and B-P-C GCL (crosslinked polymer) with the same polymer loading as the effective stress increased. For example, the B-P-A-5 maintained low hydraulic conductivity ($< 10^{-10}$ m/s) when permeated with CCR leachate at 250 kPa, whereas the hydraulic conductivity of B-P-B-5 and B-P-C-5 GCLs were still higher than 10^{-10} m/s at 500 kPa.

3.7. Mechanism controlling hydraulic conductivity of B-P GCLs with different polymer types

Based on past conceptual models for mechanisms controlling the hydraulic conductivity of B-P GCLs (Scalia IV et al., 2018; Tian et al., 2019; Norris et al., 2022), the conceptual model of the mechanisms controlling the hydraulic conductivity of B-P GCLs with different

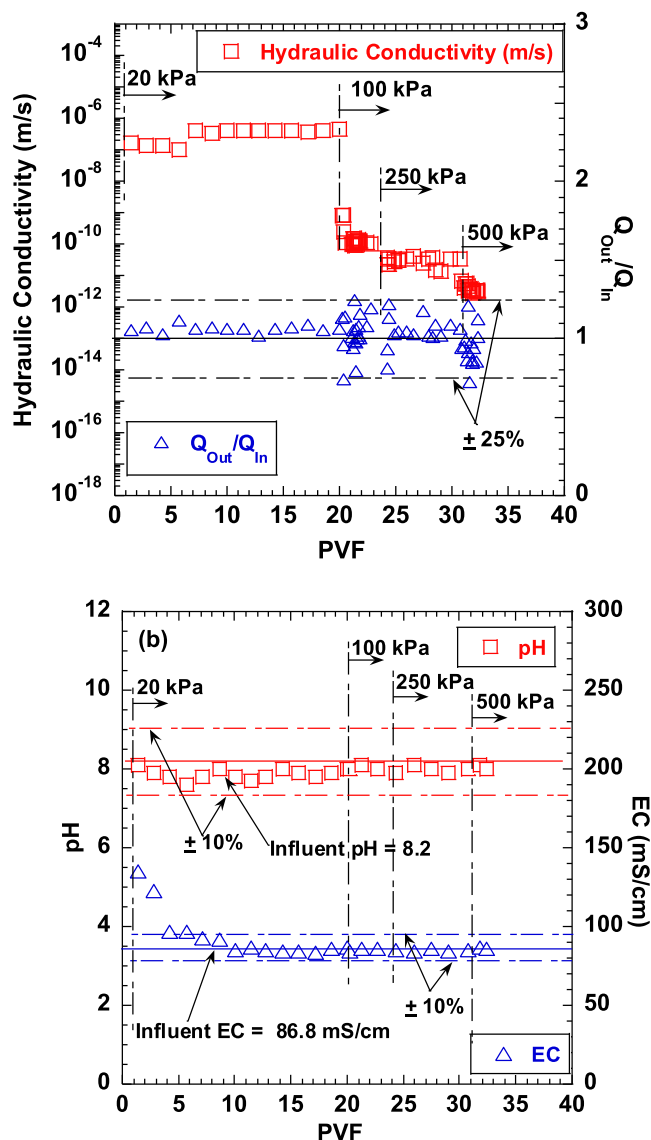


Fig. 10. Hydraulic conductivity, ratio of outflow to inflow (Q_{out}/Q_{in}), pH, and EC from test of B-P-A-5 GCL permeated with CCR leachate.

polymer types is illustrated schematically in Fig. 12. Under dry conditions, the interior of Na-B GCL consists of granular Na-B separated by relatively large intergranular pores. Permeation with very aggressive leachate ($I > 2000$ mM) significantly constrains osmotic swelling, e.g., SI for Na-B < 5 mL/2 g as shown in Fig. 1. Consequently, the intergranular pores cannot be filled up and the Na-B GCL has a high hydraulic conductivity, e.g., $K > 1 \times 10^{-7}$ m/s at normal stress of 20 kPa in Table 1, which is consistent with the report from Shackelford et al. (2000), Kolstad et al. (2004), Zainab et al. (2021), and Wireko et al. (2022).

Prior to hydration, GCLs containing dry bentonite-polymer mixtures have granules of polymer (linear, branched linear, and crosslinked) interspersed in the intergranular pores between bentonite granules. During permeation with very aggressive leachate ($I > 2000$ mM), hydrogel formed in B-P GCLs can fill in interaggregate pores, i.e., clogging mechanism, leading to a lower hydraulic conductivity compared with Na-B GCLs. The clogging mechanism in B-P GCLs has been proven and comprehensively discussed by Tian et al. (2019) and Guarena et al. (2024). As for B-P GCLs with crosslinked polymer, permeation with leachates induces the formation of a 3D matrix of

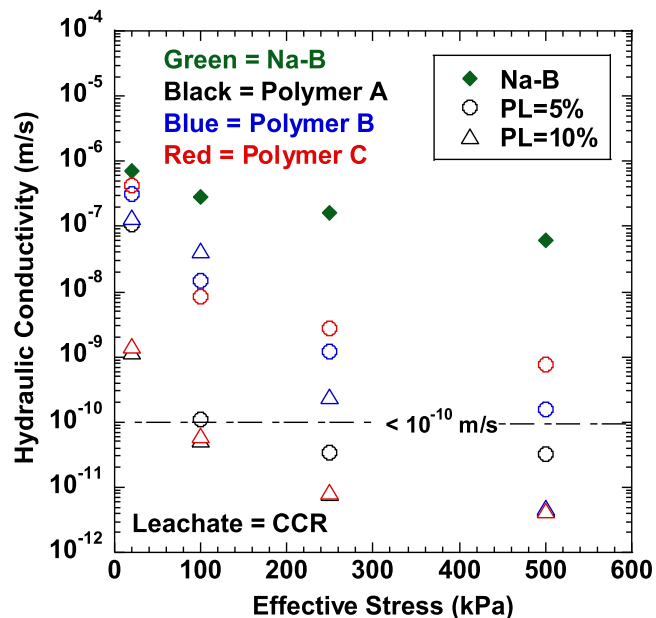


Fig. 11. Hydraulic conductivity of GCLs to synthetic leachates as a function of effective stress to CCR leachate.

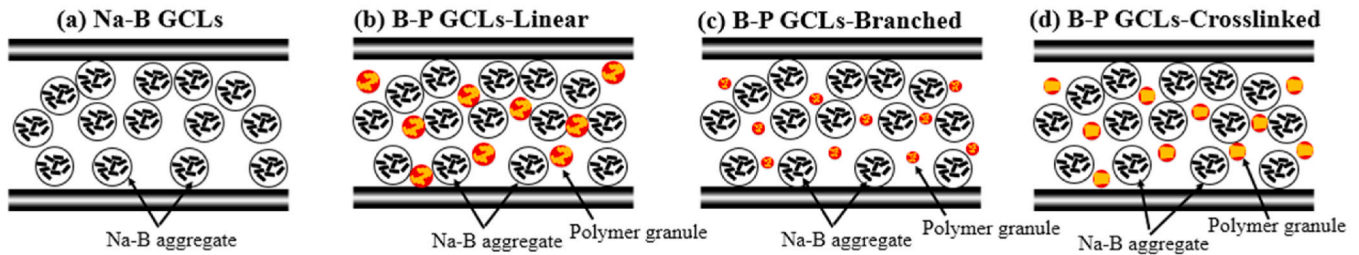
interconnected polymer hydrogel which can maintain its shape. In contrast to crosslinked polymer, linear polymers form a viscous, glue-like substance that can adsorb to the surfaces of bentonite particles, effectively entangling the bentonite together, leading to a lower pore space within the bentonite (Zainab et al., 2021; Geng et al., 2016, 2022; Norris et al., 2022; Chen et al., 2023a; 2023b). Similarly, branched polymer hydrogels may also entangle bentonite particles, leading to a decrease in the available pore space within the bentonite. In addition, the entanglement between branched polymer with clay may be stronger than that of linear polymer. This is because the side chains of the branched polymer hydrogel improve the ability to catch smaller bentonite particles (Zhang et al., 2013). The variation in clogging mechanisms governing B-P GCLs with different polymer additives is supported by the observation of minimal polymer elution but maximal viscosity in B-P GCLs containing branched linear polymer, as illustrated in Figs. 6 and 8. However, further study should be conducted to investigate the major factors of polymer retention in B-P GCLs with different polymer additives.

4. Summary and conclusions

Hydraulic conductivity of Na-B and B-P GCLs with three different polymer additives (e.g., branched, linear, crosslinked) to synthetic CCR, MSWI, and MW leachates were evaluated in this study. The mock B-P GCLs contained Na-B dry blended with polymer and had various polymer loadings ranging from 5% to 15%. The hydraulic conductivity tests were conducted at 20 kPa until reaching hydraulic and chemical equilibrium, and then the effective confining stress was increased incrementally from 20 kPa to 100 kPa, 250 kPa, and 500 kPa to mimic field conditions. Based on the findings from these tests, the following conclusions and recommendations are drawn:

- The mock Na-B GCL showed high hydraulic conductivity to synthetic CCR, MSWI, and MW leachates with an ionic strength ranging from 2127 mM to 3179 mM, illustrating that Na-B GCL may not be adequate to manage these aggressive synthetic leachates.
- Mock B-P-A GCLs with 10% branched polymer had low hydraulic conductivity ($< 1 \times 10^{-10}$ m/s) to synthetic MW and MSWI leachates at 20 kPa effective confining stress, whereas the B-P-B GCLs with

Dry State



Hydration

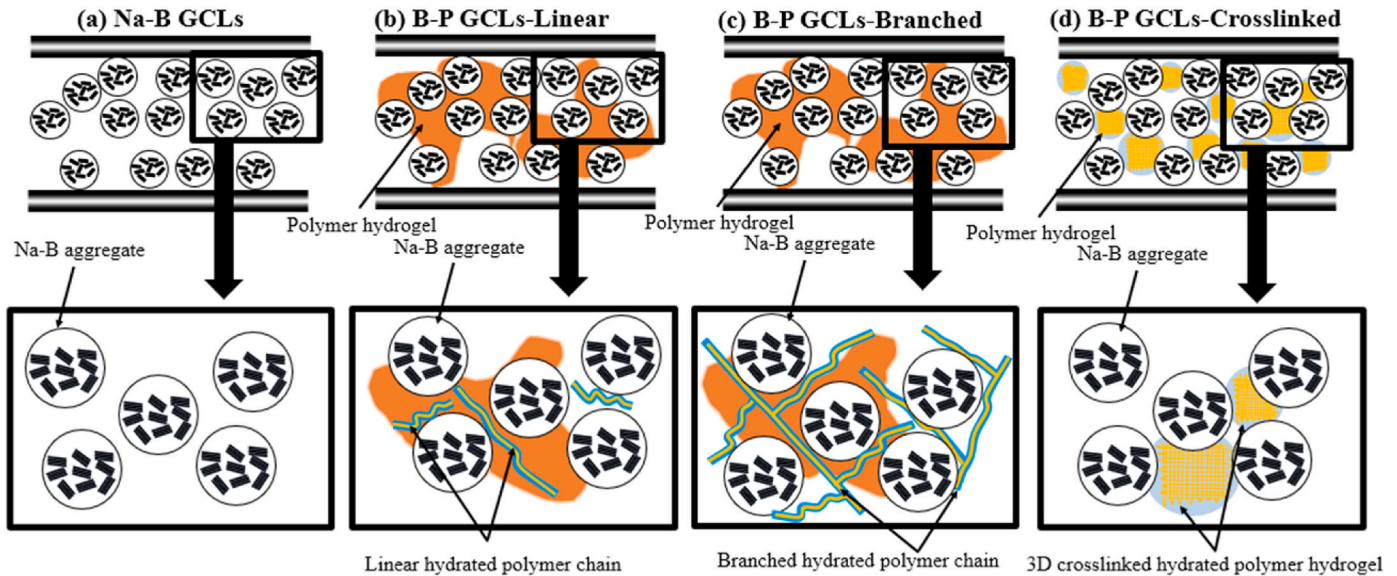


Fig. 12. The conceptual model of the mechanisms controlling the hydraulic conductivity of B-P GCLs with different polymer types.

linear polymer and B-P-C GCLs with crosslinked polymer cannot maintain low hydraulic conductivity at the same testing condition. This observation illustrates that the polymer type affects the chemical compatibility of B-P GCL.

- The B-P-A GCL permeated with synthetic CCR, MW, and MSWI leachates showed less polymer elution than that of B-P-B and B-P-C GCLs at the same testing condition. The lower polymer elution of polymer A may be attributed to the strong bonding between branched polymer and bentonite. The high polymer retention rate in B-P-A GCL let the polymer hydrogel clog the intergranular pore space effectively as the swelling of bentonite was suppressed in synthetic leachates, resulting in low hydraulic conductivity and high chemical compatibility.
- The hydraulic conductivity of all Na-B and B-P GCLs decreased as the confining stress increased. The hydraulic conductivity of B-P GCLs decreased faster than that of Na-B GCLs as the effective confining stress increased. The beneficial effect of increasing effective confining stress on the reduction in hydraulic conductivity of B-P GCLs was affected by the polymer type and polymer loading. B-P GCLs with branched polymer showed the fastest decreasing trend in

hydraulic conductivity compared to B-P GCLs with linear or cross-linked polymer.

CRediT authorship contribution statement

Dong Li: Writing – review & editing, Writing – original draft, Methodology, Investigation, Data curation. **Hanrui Zhao:** Writing – review & editing, Writing – original draft, Conceptualization. **Kuo Tian:** Writing – review & editing, Writing – original draft, Supervision.

Data availability

Data will be made available on request.

Acknowledgement

This material is based upon work supported by the Bentonite Performance Minerals LLC. Any opinions, findings and conclusions in this material are those of the authors and do not necessarily reflect the views of Bentonite Performance Minerals LLC.

Appendix

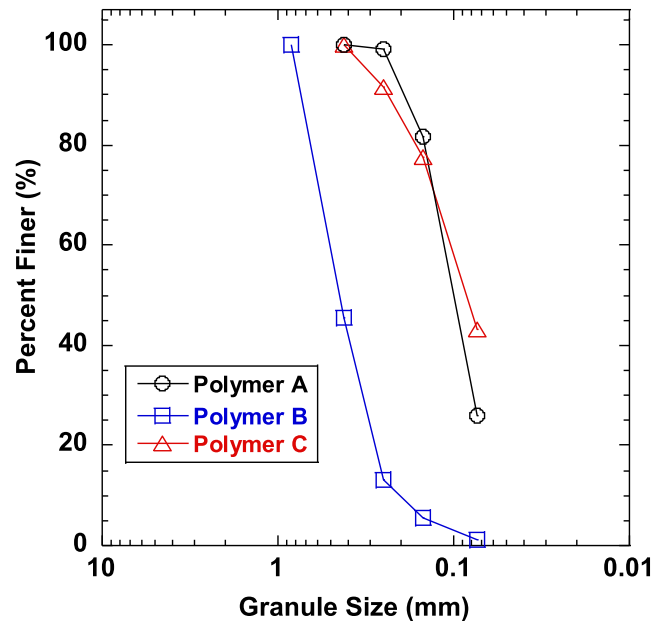


Fig. A1. Grain size distribution of polymer used in this study.

References

- Abdelaal, F.B., Rowe, R.K., Smith, M., Thiel, R., 2011. OIT depletion in HDPE geomembranes used in contact with solutions having very high and low pH. In: Proceedings of the 14th Pan-American Conference of Soil Mechanics and Geotechnical Engineering, Toronto, Ont, pp. 2–6.
- ASTM D 1193. Standard Specification for Reagent Water, ASTM International, West Conshohocken, Pennsylvania, USA.
- ASTM D 5890. Standard Test Method for Swell Index of Clay Mineral Component of Geosynthetic Clay Liners, ASTM International, West Conshohocken, Pennsylvania, USA.
- ASTM D 6766. Standard Test Method for Evaluation of Hydraulic Properties of Geosynthetic Clay Liners Permeated with Potentially Incompatible Aqueous Solutions, ASTM International, West Conshohocken, Pennsylvania, USA.
- ASTM D 7348. Standard Test Methods for Loss on Ignition (LOI) of Solid Combustion Residues, ASTM International, West Conshohocken, Pennsylvania, USA.
- Ashmawy, A.K., El-Hajji, D., Sotelo, N., Muhammad, N., 2002. Hydraulic performance of untreated and polymer-treated bentonite in inorganic landfill leachates. *Clay Clay Miner.* 50 (5), 546–552.
- Athanassopoulos, C., Benson, C., Chen, J., Donovan, M., 2015. Hydraulic conductivity of a polymer-modified GCL permeated with high-pH solutions. In: Proceedings of the Geosynthetics.
- Bouazza, A., 2002. Geosynthetic clay liners. *Geotext. Geomembranes* 20 (1), 3–17.
- Bouazza, A., Rouf, M.A., Singh, R.M., Rowe, R.K., Gates, W.P., 2017. Gas diffusion and Permeability for geosynthetic clay liners with powder and granular bentonites. *Geosynth. Int.* 24 (6), 604–614.
- Bradshaw, S.L., Benson, C.H., 2014. Effect of municipal solid waste leachate on hydraulic conductivity and exchange complex of geosynthetic clay liners. *J. Geotech. Geoenviron. Eng.* 140 (4), 04013038.
- Bradshaw, S.L., Benson, C.H., Rauen, T.L., 2016. Hydraulic conductivity of geosynthetic clay liners to recirculated municipal solid waste leachates. *J. Geotech. Geoenviron. Eng.* 142 (2), 04015074.
- Caminade, A.M., Beraa, A., Laurent, R., Delavaux-Nicot, B., Hajjaji, M., 2019. Dendrimers and hyper-branched polymers interacting with clays: fruitful associations for functional materials. *J. Mater. Chem. A* 7 (34), 19634–19650.
- Chatterji, J., Borchardt, J.K., 1981. Applications of water-soluble polymers in the oil field. *Appl. water-soluble. Polym. oil. field* 33 (11), 2042–2056.
- Chen, J.N., Benson, C.H., Edil, T.B., 2018. Hydraulic conductivity of geosynthetic clay liners with sodium bentonite to coal combustion product leachates. *J. Geotech. Geoenviron. Eng.* 144 (3), 04018008.
- Chen, J.N., Salihoglu, H., Benson, C., Likos, W., Edil, T., 2019. Hydraulic conductivity of bentonite-polymer composite geosynthetic clay liners permeated with coal combustion product leachates. *J. Geotech. Geoenviron. Eng.* 145 (9), 04019038.
- Chen, X., Tan, Y., Chen, J., Peng, D., Huang, T., Meng, C., 2023a. Hydraulic conductivity and multi-scale pore structure of polymer-enhanced geosynthetic clay liners permeated with bauxite liquors. *Geotext. Geomembranes* 52 (1), 46–58.
- Chen, X., Tan, Y., Copeland, T., Chen, J., Peng, D., Huang, T., 2023b. Polymer elution and hydraulic conductivity of polymer-bentonite geosynthetic clay liners to bauxite liquors. *Appl. Clay Sci.* 242, 107039.
- Devrani, S., Sharma, R., Rajesh, M.P., Kapoor, A., 2017. Exploring viscoelastic characteristics of polymer-water solutions by viscometric analysis. *Asian J. Chem.* 29, 1953–1958.
- Di Emidio, G., Mazzieri, F., Verastegui-Flores, R.D., Van Impe, W., Bezuijen, A., 2015. Polymer-treated bentonite clay for chemical-resistant geosynthetic clay liners. *Geosynth. Int.* 22 (1), 125–137.
- Donovan, M.S., Valorio, R., Gebka, B., 2017. Polymer enhanced geosynthetic clay liners for bauxite storage. In: Proceedings of the 35th International ICSOBA Conference, Hamburg, Germany. ICSOBA Travaux, Quebec, Canada, pp. 469–478.
- Gao, C., 2013. Viscosity of partially hydrolyzed polyacrylamide under shearing and heat. *J. Pet. Explor. Prod. Technol.* 3 (3), 203–206.
- Geng, W., Likos, W.J., Benson, C.H., 2016. Viscosity of polymer-modified bentonite as a hydraulic performance index. In: Geo-Chicago 2016, pp. 498–507.
- Geng, W., Salihoglu, H., Likos, W.J., Benson, C.H., 2022. Index tests for geosynthetic clay liners containing bentonite-polymer composites. *Enviro. Geotech.* 40 (XXXX), 1–12.
- Ghazizadeh, S., Bareither, C.A., Scalia, J., Shackelford, C.D., 2018. Synthetic mining solutions for laboratory testing of geosynthetic clay liners. *J. Geotech. Geoenviron. Eng.* 144 (10), 06018011.
- Guarena, N., Dominijanni, A., Manassero, M., 2024. Pore-scale mechanisms underlying the behavior of enhanced bentonites exposed to aggressive inorganic solutions. *Appl. Clay Sci.* 251, 107318.
- Guler, E., Ozhan, H.O., Karaoglu, S., 2018. Hydraulic performance of anionic polymer-treated bentonite-granular soil mixtures. *Appl. Clay Sci.* 157, 139–147.
- Gustitus, S.A., Nguyen, D., Chen, J.N., Benson, C.H., 2021. Quantifying polymer loading in bentonite-polymer composites using loss on ignition and total carbon analyses. *Geotech. Test J.* 44 (5), 1–19.
- Jo, H.Y., Katsumi, T., Benson, C.H., Edil, T.B., 2001. Hydraulic conductivity and swelling of nonprehydrated GCLs permeated with single-species salt solutions. *J. Geotech. Geoenviron. Eng.* 127 (7), 557–567.
- Jo, H.Y., Benson, C.H., Shackelford, C.D., Lee, J.M., Edil, T.B., 2005. Long-term hydraulic conductivity of a geosynthetic clay liner permeated with inorganic salt solutions. *J. Geotech. Geoenviron. Eng.* 131 (4), 405–417.
- Katsumi, T., Ishimori, H., Onikata, M., Fukagawa, R., 2008. Long-term barrier performance of modified bentonite materials against sodium and calcium permeant solutions. *Geotext. Geomembranes* 26 (1), 14–30.
- Kolstad, D.C., Benson, C.H., Edil, T.B., 2004. Hydraulic conductivity and swell of nonprehydrated geosynthetic clay liners permeated with multispecies inorganic solutions. *Geotext. Geomembranes* 130, 1236–1249.
- Koerner, R.M., 2012. Designing with Geosynthetics, sixth ed., Vol.2. Xlibris Corporation, Bloomington, IN, USA.
- Li, D., Zainab, B., Tian, K., 2021. Effect of effective stress on hydraulic conductivity of bentonite-polymer geosynthetic clay liners to coal combustion product leachates. *Enviro. Geotech.* <https://doi.org/10.1680/jenge.21.00077>.

- Li, Q., Chen, J.N., Benson, C.H., Peng, D., 2021. Hydraulic conductivity of bentonite-polymer composite geosynthetic clay liners permeated with bauxite liquor. *Geotext. Geomembranes* 49 (2), 420–429.
- Mazzieri, F., Emidio, G.D., 2015. Hydraulic conductivity of a dense prehydrated geosynthetic clay liner. *Geosynth. Int.* 22 (1), 138–148.
- McKeen, L.W., 2017. *Film Properties of Plastics and Elastomers*. William Andrew.
- McWatters, S., Rowe, R.K., Di Battista, V., Sfilijog, B., Wilkins, D., Spedding, T., 2019. Exhumation and performance of a composite barrier system in Antarctica after 4 years exposure. *Can. Geotech. J.* 57 (8), 1130–1152.
- Mitchell, J.K., Soga, K., 1993. *Fundamentals of Soil Behavior*, second ed. John Wiley & Sons, Inc., New York.
- Norris, A., Aghazamani, N., Scalia, J., Shackelford, C.D., 2022. Hydraulic performance of geosynthetic clay liners comprising anionic polymer-enhanced bentonites. *J. Geotech. Geoenviron. Eng.* 148 (6), 04022039.
- Norrish, K., Quirk, J.P., 1954. Crystalline swelling of montmorillonite: use of electrolytes to control swelling. *Nature* 173, 255–256.
- Özhan, H.O., 2018. Hydraulic capability of polymer-treated GCLs in saline solutions at elevated temperatures. *Appl. Clay Sci.* 161, 364–373.
- Prongmanee, N., Chai, J.C., 2019. Performance of geosynthetic clay liner with polymerized bentonite in highly acidic or alkaline solutions. *Int.J.Geosynth.Ground Eng.* 5, 1–11.
- Rivas, B.L., Urbano, B.F., Sánchez, J., 2018. Water-soluble and insoluble polymers, nanoparticles, nanocomposites and hybrids with ability to remove hazardous inorganic pollutants in water. *Front. Chem.* 6, 1–13.
- Salihoglu, H., Chen, J.N., Likos, W.J., Benson, C.H., 2016. Hydraulic Conductivity of Bentonite-Polymer Geosynthetic Clay Liners in Coal Combustion Product Leachates. *Proceedings of the Geo-Chicago 2016: Sustainable Geoenvironmental Systems*, Chicago, IL, USA, ASCE, Reston, VA, USA, pp. 438–447.
- Setz, M.C., Tian, K., Benson, C.H., Bradshaw, S.L., 2017. Effect of ammonium on the hydraulic conductivity of geosynthetic clay liners. *Geotext. Geomembranes* 45 (6), 665–673.
- Scalia IV, J., Benson, C.H., Bohnhoff, G.L., Edil, T.B., Shackelford, C.D., 2014. Long-term hydraulic conductivity of a bentonite-polymer composite permeated with aggressive inorganic solutions. *J. Geotech. Geoenviron. Eng.* 140 (3), 04013025.
- Scalia IV, J., Bohnhoff, G.L., Shackelford, C.D., Benson, C.H., Sample-Lord, K.M., Malusis, M.A., Likos, W.J., 2018. Enhanced bentonites for containment of inorganic waste leachates by GCLs. *Geosynth. Int.* 25 (4), 392–411.
- Shackelford, C.D., Benson, C.H., Katsumi, T., Edil, T.B., Lin, L., 2000. Evaluating the hydraulic conductivity of GCLs permeated with non-standard liquids. *Geotext. Geomembranes* 18, 133–162.
- Singh, C., Balazs, A.C., 2000. Effect of polymer architecture on the miscibility of polymer/clay mixtures. *Polym. Int.* 49 (5), 469–471.
- Tian, K., Benson, C.H., Likos, W.J., 2016. Hydraulic conductivity of geosynthetic clay liners to low-level radioactive waste leachate. *J. Geotech. Geoenviron. Eng.* 142 (8), 04016037.
- Tian, K., Benson, C.H., Likos, W.J., 2017. Effect of an anion ratio on the hydraulic conductivity of a bentonite-polymer geosynthetic clay liner. In: *Geotechnical Frontiers 2017*, pp. 180–189.
- Tian, K., Benson, C.H., 2018. Containing Bauxite Liquor Using Bentonite-Polymer Composite Geosynthetic Clay Liners: towards a Sustainable Geoenvironment. *Proceedings of the 8th International Congress on Environmental Geotechnics*.
- Tian, K., Likos, W.J., Benson, C.H., 2019. Polymer elution and hydraulic conductivity of bentonite-polymer composite geosynthetic clay liners. *J. Geotech. Geoenviron. Eng.* 145 (10), 04019071.
- Townsend, T.G., Meeroff, D.E., Darioosh, R., Moody, C., Wally, J., 2015. Assessing options for on-site leachate management at Florida landfills. *Hinkley.Cent.Sol. Hazard.Waste Manag.*
- Vryzas, Z., Kelessidis, V.C., Nalbantian, L., Zaspalis, V., Gerogiorgis, D.I., Wubulikasimu, Y., 2017. Effect of temperature on the rheological properties of neat aqueous Wyoming sodium bentonite dispersions. *Appl. Clay Sci.* 136, 26–36.
- Williams, P.A., 2007. *Handbook of Industrial Water Soluble Polymers*. Blackwell Publishing Ltd, Oxford, UK. <https://doi.org/10.1002/9780470988701>.
- Wireko, C., Zainab, B., Tian, K., Abichou, T., 2020. Effect of specimen preparation on the swell index of bentonite-polymer GCLs. *Geotext. Geomembranes* 48 (6), 875–885.
- Wireko, C., Abichou, T., 2021. Investigating factors influencing polymer elution and the mechanism controlling the chemical compatibility of GCLs containing linear polymers. *Geotext. Geomembranes* 49 (4), 1004–1018.
- Wireko, C., Abichou, T., Tian, K., Zainab, B., Zhang, Z., 2022. Effect of incineration ash leachates on the hydraulic conductivity of bentonite-polymer composite geosynthetic clay liners. *Waste Manag.* 139, 25–38.
- Xue, L., Agarwal, U.S., Lemstra, P.J., 2005. Shear degradation resistance of star polymers during elongational flow. *Macromolecules* 38 (21), 8825–8832.
- Zainab, B., Tian, K., 2020. Hydraulic Conductivity of Bentonite-Polymer Geosynthetic Clay Liners to Coal Combustion Product Leachates. *Geo-Congress 2020*. ASCE, Minneapolis, MN, USA, pp. 579–586.
- Zainab, B., Wireko, C., Dong, L., Tian, K., Tarek, K., 2021. Hydraulic conductivity of bentonite-polymer geosynthetic clay liners to coal combustion product leachates. *Geotext. Geomembranes* 49 (5), 1129–1138.
- Zhang, B., Su, H., Gu, X., Huang, X., Wang, H., 2013. Effect of structure and charge of polysaccharide flocculants on their flocculation performance for bentonite suspensions. *Colloids Surf. A Physicochem. Eng. Asp.* 436, 443–449.